

SACLANTCEN MEMORANDUM  
serial no.: SM-271

SACLANT UNDERSEA  
RESEARCH CENTRE

SACLANT ASW RESEARCH CENTRE  
LIBRARY COPY #5

MEMORANDUM



**Scattering from a rough  
sedimental seafloor containing  
shear and layering, as determined  
by perturbation theory**

H.-H. Essen

July 1993

The SACLANT Undersea Research Centre provides the Supreme Allied Commander Atlantic (SACLANT) with scientific and technical assistance under the terms of its NATO charter, which entered into force on 1 February 1963. Without prejudice to this main task – and under the policy direction of SACLANT – the Centre also renders scientific and technical assistance to the individual NATO nations.

---

This document is released to a NATO Government at the direction of SACLANT Undersea Research Centre subject to the following conditions:

- The recipient NATO Government agrees to use its best endeavours to ensure that the information herein disclosed, whether or not it bears a security classification, is not dealt with in any manner (a) contrary to the intent of the provisions of the Charter of the Centre, or (b) prejudicial to the rights of the owner thereof to obtain patent, copyright, or other like statutory protection therefor.
- If the technical information was originally released to the Centre by a NATO Government subject to restrictions clearly marked on this document the recipient NATO Government agrees to use its best endeavours to abide by the terms of the restrictions so imposed by the releasing Government.

---

Page count for SM-271  
(excluding Covers  
and Data Sheet)

Pages	Total
i-vi	6
1-21	21
	<hr/>
	27

---

SACLANT Undersea Research Centre  
Viale San Bartolomeo 400  
19138 San Bartolomeo (SP), Italy

tel: 0187 540 111  
fax: 0187 524 600  
telex: 271148 SACENT I

NORTH ATLANTIC TREATY ORGANIZATION

SACLANTCEN SM-271

Scattering from a rough sedimental  
seafloor containing shear  
and layering, as determined  
by perturbation theory

H.-H. Essen

---

The content of this document pertains  
to work performed under Project 23 of  
the SACLANTCEN Programme of Work.  
The document has been approved for  
release by The Director, SACLANTCEN.

Issued by:  
Underwater Research Division



H. Urban  
Division Chief

SACLANTCEN SM-271

SACLANTCEN SM-271

**Scattering from a rough sedimental  
seafloor containing shear and layering,  
as determined by perturbation theory**

H.-H. Essen

**Executive Summary:** Sound scattering from the seafloor is of great importance for sonar performance. This is not only valid for the estimation of reverberation, limiting acoustic ranges, but also for detecting mines by acoustic means. While the first task mainly concerns low frequencies, the latter demands high frequencies.

A large number of high-frequency backscatter experiments has been performed over the past 30 years. However the basic scattering mechanisms are still not completely understood. Scattering models have been derived by considering two different processes: scattering from bottom roughness and volume scattering from inhomogeneities within the seafloor. From observations there is some evidence that the latter process is dominant for soft seafloors (mud, silt), while bottom roughness is sufficient to explain backscatter from harder seafloors (sand). Furthermore, for grazing angles below the critical angle of total reflection (some  $30^\circ$  for a sandy seafloor), sound penetration into the bottom is low, and volume scattering can be ignored.

In a recent SACLANTCEN Report, Essen (1992) showed that important features of observed backscatter from sandy seafloors may be explained by first-order perturbation theory with reasonable assumptions on bottom roughness. The seafloor model used so far (homogeneous fluid halfspace) obviously oversimplifies reality. In this memorandum, the seafloor is allowed to be shear-supporting or to be layered (without shear). For grazing angles below critical, significant modification of backscatter strength is obtained if the shear-wave velocity exceeds some  $350 \text{ ms}^{-1}$ . Layering mainly influences backscatter angles just above critical.

Scattering strengths, as derived by perturbation theory, crucially depend on the roughness spectrum of the seafloor. Detailed knowledge is required to allow for quantitative comparison of experimental results against theory. In the case of high frequencies, the respective two-dimensional roughness spectrum may, and should be, measured by means of stereo photography.



SACLANTCEN SM-271

**Scattering from a rough sedimental  
seafloor containing shear and layering,  
as determined by perturbation theory**

H.-H. Essen

**Abstract:** First-order perturbation theory is applied to reverberation from a rough sedimental seafloor. In addition to existing approaches, the seafloor is allowed to be shear-supporting or to be layered. Scattering strengths are derived for both monostatic and bistatic reverberation, and compared with results from a non-layered fluid bottom. By exceeding some  $350 \text{ ms}^{-1}$ , shear-wave velocity significantly influences scattering strength for angles below the critical angle of total reflection. Layering, as modelled by a two-layer fluid seafloor, mainly influences scattering at grazing angles just above critical.

**Keywords:** acoustic reverberation ◦ layered seafloor ◦ perturbation theory  
◦ rough seafloor ◦ shear waves

## Contents

1. Introduction . . . . .	1
2. Perturbation theory . . . . .	4
3. Numerical results for backscatter . . . . .	9
4. Numerical results for bistatic scattering . . . . .	16
5. Conclusions . . . . .	19
References . . . . .	21



# 1

## Introduction

---

Bottom reverberation is of considerable importance in underwater acoustics. During the past 30 years a large number of backscatter experiments has been performed. Two articles by Stanic et al. (1988, 1989) provide short reviews and references on high-frequency results. The interpretation of experimental data is difficult, however, and no final theory is yet available. As suggested by Mackenzie (1961), the dependence of backscatter strength on grazing angle may, in many cases, be described by Lambert's Rule (e.g. Boehme and Chotiros, 1988; Ellis and Crowe, 1991). The advantage of this approach is that the experimental results may be summarized by only one parameter, e.g. the backscattering strength at normal incidence, which adjusts the theoretical curve to measured backscattering strengths and may be frequency dependent. The disadvantage is that Lambert's Rule may not be derived from physical processes, relating backscattering strength to seafloor parameters.

Physical processes assumed to cause bottom reverberation are scattering from seafloor roughness or inhomogeneities within the sedimental seafloor. Investigations by Jackson et al. (1986, 1992) show that the first mechanism is dominant for sandy seafloors. The scattering model used is based on the first-order perturbation theory of Kuo (1964) considering a fluid/fluid interface described by the ratios of density and sound-velocity of sediment versus water and allowing for attenuation of sound in the sediment.

An extensive literature exists on scattering from rough surfaces. A recent review of mainly theoretical work is given by Ogilvy (1991). Most of the scattering theories are based on idealized boundary conditions, i.e. assume a pressure release (Dirichlet boundary condition) or an ideally rigid surface (Neumann boundary condition), both of which are not appropriate for scattering from the seafloor (cf. Essen, 1992). Realistic boundary conditions, i.e. continuity of pressure and normal component of particle velocity, may be considered by perturbation theory. A summary of the respective literature is presented by Jackson et al. (1986).

Perturbation theory is only valid when roughness amplitudes are small compared to acoustic wavelength. While this requirement often holds for the scattering component itself, it may fail for the roughness field represented by the total spectrum. In this case, composite (two-scale) models can be used, extending the applicability of perturbation theory to more general conditions (cf. Jackson et al., 1986). Thorsos (1990) compares different theoretical approaches to acoustic scattering from a rough sea surface of known statistics and finds reasonable results from perturbation theory even when roughness amplitudes are of the order of the acoustic wavelength.

Perturbation theory yields the three-dimensional scattering strength, describing the dependence on grazing angle and azimuthal angle of the incident and scattered energy. Seafloor parameters involved are the two-dimensional roughness spectrum and the ratios of sound velocity and density of sediment versus water. As most measurements are backscatter only, comparison of predicted and measured data has to be restricted to this special case. Mainly in the case of sandy bottoms, perturbation theory explains important features of measured backscattering strength, which are its absolute value, its dependence on grazing angle and frequency. The critical angle of total reflection for sandy seafloors is about  $30^\circ$ . For grazing angles smaller than critical, the acoustic field decays exponentially within the bottom and the influence of volume scattering can be assumed to be negligible.

For quantitative comparison of theoretical and experimental results, the roughness spectrum has to be known. Two papers (Stanic et al. 1989; Jackson and Briggs, 1992), referring to sandy seafloors, contain this information from stereo photography. Predicted and observed backscattering strengths agree reasonably. Perturbation theory yields a  $\sin^4$  dependence of backscatter for small grazing angles, and a cusp at the critical angle. By applying a composite model the dependence on grazing angle is smoothed, and reasonable agreement with Lambert's Rule may be obtained for grazing angles between about  $5^\circ$  and  $40^\circ$ . As pointed out by Essen (1992), some backscatter measurements reported in the literature show evidence for the predicted cusp at critical angle. For grazing angles, exceeding some  $40^\circ$  observed backscattering strengths show a strong rise with increasing angle, which is in accordance with perturbation theory but not with Lambert's Rule.

Even though some measurements showing a linear increase of backscatter with frequency, most measured data are frequency independent (cf. Urick, 1983). To reproduce this feature by the theoretically derived scattering coefficients, the one-dimensional roughness spectrum has to decay with wavenumber by  $k^{-3}$ , while a  $k^{-2}$  dependence yields a linear increase of the backscatter coefficient with frequency. There is some evidence from observations that roughness spectra at the wavelength range 1–10 cm show a power-law dependence  $k^{-n}$  with  $n$  ranging between 2 and 3.

It is obvious that the homogeneous fluid seafloor model is oversimplified. In this paper, the influence of two additional properties is investigated. The first property is shear, which is an important parameter for sandy sediments (cf. Hamilton, 1980). In unconsolidated sediments, shear-wave velocity is small as compared to compressional wave velocity but of some influence on the seafloor reflectivity. Applying the first-order perturbation approach, the influence of shear as well as layering on mono- and bistatic reverberation is investigated. The presence of shear mainly affects scattering strength for grazing angles below critical, while a layered seafloor influences scattering strength for grazing angles above critical.

Theoretical investigations are carried out with regard to a frequency range 10–100 kHz. Roughness spectra with  $k^{-2}$  and  $k^{-3}$  decay and a suitable low-wavenumber cutoff are considered. This model is appropriate to demonstrate the influence of

SACLANTCEN SM-271

shear and layering on scattering strength and complications are avoided, which arise with the extension of the fractal feature of the spectrum to wavenumbers much smaller than the acoustic ones.

# 2

## Perturbation theory

---

This section contains a short presentation on first-order perturbation theory applied to acoustic scattering from a rough seafloor. A cartesian coordinate system  $(\mathbf{x}, x_3)$  is used with the mean surface in the plane  $x_3 = 0$ , and  $x_3$  pointing upwards. Throughout, bold letters represent two-dimensional horizontal vectors. For simplicity the incident acoustic field is assumed to be a plane wave represented by the potential of the particle displacement ( $\phi$ ),

$$\phi_0 = A_0 \exp[i(\mathbf{k}_0 \cdot \mathbf{x} - \gamma_{w0} x_3 - \omega t)], \quad (1)$$

where  $\mathbf{k}_0 = (\omega/c_w) \cos(\vartheta_0)[\cos(\varphi_0), \sin(\varphi_0)]$  is the horizontal wavenumber vector and  $\gamma_{w0} = (\omega/c_w) \sin(\vartheta_0)$  the vertical component,  $\omega$  is the circular frequency and  $c_w$  the sound velocity of sea water. Horizontal (azimuthal) angles ( $\varphi$ ) are measured anticlockwise from the  $x_1$  axis, and vertical angles ( $\vartheta$ ) from the surface, i.e. they are grazing angles. Acoustic pressure ( $p$ ) and particle displacements ( $u, u_3$ ) depend on the potential  $\phi$  by

$$p = \rho_w \frac{\partial^2 \phi}{\partial t^2}, \quad u_i = \frac{\partial \phi}{\partial x_i}, \quad i = 1, 2, 3, \quad (2)$$

where  $\rho_w$  is the density of sea water.

The bottom roughness is described by  $x_3 = \zeta(\mathbf{x})$  and represented by a two-dimensional Fourier integral

$$\zeta = \int Z(\mathbf{k}) \exp[i(\mathbf{k} \cdot \mathbf{x})] d\mathbf{k}, \quad \text{with } Z(-\mathbf{k}) = Z^*(\mathbf{k}). \quad (3)$$

The constraint on the Fourier amplitudes  $Z$  is introduced for causing real values  $\zeta$  and is appropriate for the frozen seafloor. Different from a moving sea surface, waves of opposite direction need not be distinguished.

For application in scattering theory, the seafloor is assumed to be a zero-mean homogeneous random process,

$$\langle Z(\mathbf{k}) \rangle = 0, \quad \langle Z(\mathbf{k}) Z^*(\mathbf{k}') \rangle = F(\mathbf{k}) \delta(\mathbf{k} - \mathbf{k}'). \quad (4)$$

The angle brackets indicate ensemble means. The decorrelation of the Fourier amplitudes follows from the assumption of homogeneity. In this case the covariance function depends on the spatial lag between positions only and not on the position

SACLANTCEN SM-271

itself, and is the two-dimensional Fourier transform of the variance spectrum  $F(\mathbf{k})$ . The total variance of the roughness field is determined by (3) and (4):

$$\langle \zeta^2 \rangle = \int F(\mathbf{k}) d\mathbf{k}. \quad (5)$$

For application in acoustic scattering, ensemble averaging has to be replaced by spatial averaging. Implications on the necessary extension of the illuminated area are discussed by Essen (1992).

Considering a rough seafloor, approximate solutions for the scattered acoustic field may be obtained by means of perturbation theory. It is assumed that the field variables can be expanded into convergent perturbation series, e.g. the displacement potential in the water column,

$$\phi_w = \phi_w^{(0)} + \phi_w^{(1)} + \dots \quad (6)$$

The convergence is guaranteed by the existence of a small perturbation parameter, of which the power determines the perturbation order, cf. Essen (1992). The zero-order solution is obtained by applying the boundary conditions for an undisturbed seafloor, yielding a specular reflected wave in the water column,

$$\phi_w^{(0)} = [A_0 \exp(-i\gamma_{w0}x_3) + A_r \exp(i\gamma_{w0}x_3)] \exp[i(\mathbf{k}_0 \cdot \mathbf{x} - \omega t)]. \quad (7)$$

The reflected amplitude  $A_r$  depends on the seafloor model. Considering nonlinear terms in the boundary conditions and inserting the perturbation series of the field variables involved, first-order boundary conditions are obtained by accounting for quadratic coupling between zero-order acoustic variables and the bottom-roughness. The scattered acoustic field in the water column becomes

$$\phi_w^{(1)} = \int B_r \exp[i(\mathbf{k}_s \cdot \mathbf{x} + \gamma_{s0}x_3 - \omega t)] Z(\mathbf{k}) d\mathbf{k}, \quad \text{with } \mathbf{k}_s = \mathbf{k}_0 + \mathbf{k}, \quad (8)$$

with  $\gamma_{s0} = \sqrt{(\omega/c_w)^2 - k_s^2}$  (due to the wave equation). As the integration extends over  $\mathbf{k}$  of opposite signs, contributions in (8) refer to the sum and the difference of interacting wavenumbers. Again, the scattered amplitude  $B_r$  depends on the seafloor model and solutions will be presented later.

In order to compute scattered intensities, time averaging is performed by taking the squared absolute value of (8), as well as ensemble averaging (4) over the random seafloor (3),

$$I_s = \langle |\phi_w^{(1)}|^2 \rangle = \int |B_r|^2 F(\mathbf{k}) d\mathbf{k}, \quad \text{with } \mathbf{k} = \mathbf{k}_s - \mathbf{k}_0. \quad (9)$$

The scattering coefficient  $S$ , also referred to as dimensionless cross-section (cf. Jackson et al., 1986), is defined by, cf. Brekhovskikh and Lysanov (1991),

$$I_s = A_0^2 \int \frac{S}{r^2} d\mathbf{a}, \quad (10)$$

where  $r$  is the distance from the scattering area to the reference point, which is assumed to be in the far field. The integration is carried out over a sufficiently extended area to allow independent scattering from a great number of subsections. For geometrical reasons, the integral (10) may be changed to

$$I_s = A_0^2 \iint S \cot(\vartheta_s) d\varphi_s d\vartheta_s. \quad (11)$$

Transforming the integral (9) to the same variables as used in (11) and comparing the integrands, the scattering coefficient becomes

$$S(\omega, \varphi_0, \vartheta_0, \varphi_s, \vartheta_s) = \frac{\omega^2 |B_r|^2}{c_w^2 |A_0|^2} F(\mathbf{k}_s - \mathbf{k}_0) \sin^2(\vartheta_s). \quad (12)$$

Seafloor containing shear Appropriate field variables describing acoustic propagation in an elastic medium are particle displacement ( $u_i$ ) and the stress tensor ( $\tau_{ij}$ ), which can be represented by a scalar ( $\phi$ ) and a vector potential ( $\psi_i$ ),

$$u_i = \frac{\partial \phi}{\partial x_i} + \epsilon_{ijk} \frac{\partial \psi_k}{\partial x_j}, \quad i = 1, 2, 3,$$

$$\tau_{ij} = \rho \left[ (c_p^2 - 2c_t^2) \delta_{ij} \frac{\partial u_k}{\partial x_k} + c_t^2 \left( \frac{\partial u_i}{\partial x_j} + \frac{\partial u_j}{\partial x_i} \right) \right], \quad i, j = 1, 2, 3, \quad (13)$$

where  $c_p$  and  $c_t$  are the compressional- and shear-wave velocity,  $\epsilon_{ijk}$  and  $\delta_{ij}$  the permutation and Kronecker symbol, respectively. Summation has to be performed over double indices. Within the water column, the shear-wave velocity vanishes and with it the vector potential. The stress tensor reduces to equal diagonal components, representing the pressure. The boundary conditions for different media are continuity of the normal components of displacement and tangential stresses.

In the case of zero-order perturbation, i.e., an undisturbed boundary, continuity at  $x_3 = 0$  is required for

$$u_3^{(0)}, \quad \tau_{3i}^{(0)}, \quad i = 1, 2, 3. \quad (14)$$

Due to the wave equations the transmitted waves in the seafloor become

$$\phi_b^{(0)} = A_p \exp[i(\mathbf{k}_0 \cdot \mathbf{x} - \gamma_{p0} x_3 - \omega t)],$$

$$\psi_{bi}^{(0)} = A_{ti} \exp[i(\mathbf{k}_0 \cdot \mathbf{x} - \gamma_{t0} x_3 - \omega t)], \quad i = 1, 2, 3, \quad (15)$$

with  $\gamma_{p0} = \sqrt{(\omega/c_p)^2 - k_0^2}$  and  $\gamma_{t0} = \sqrt{(\omega/c_t)^2 - k_0^2}$ . By setting  $A_{t3} = 0$  and defining  $k_0 A_t = k_{02} A_{t1} - k_{01} A_{t2}$ , the boundary conditions yield

$$\mathbf{C}_0(A_r, A_p, A_t)^T = (\gamma_{w0} A_0, -\rho_w \omega^2 A_0, 0)^T, \quad (16)$$

SACLANTCEN SM-271

where

$$\mathbf{C}_0 = \begin{pmatrix} \gamma_{w0} & \gamma_{p0} & k_0 \\ \rho_w \omega^2 & \rho_b(2c_t^2 k_0^2 - \omega^2) & -2\rho_b c_t^2 k_0 \gamma_{t0} \\ 0 & 2\rho_b c_t^2 k_0 \gamma_{p0} & \rho_b(2c_t^2 k_0^2 - \omega^2) \end{pmatrix},$$

and where  $\rho_b$  is the density of the seafloor.

For first-order perturbation solutions quadratic coupling between the zero-order acoustic and the roughness field has to be considered. Quadratic terms occur from the slopes of the rough seafloor and by expanding the boundary conditions for the undisturbed interface. Continuity is required at  $x_3 = 0$  for

$$\begin{aligned} u_3 - u_1 \frac{\partial \zeta}{\partial x_1} - u_2 \frac{\partial \zeta}{\partial x_2} + \frac{\partial u_3}{\partial x_3} \zeta, \\ \tau_{3i} - \tau_{1i} \frac{\partial \zeta}{\partial x_1} - \tau_{2i} \frac{\partial \zeta}{\partial x_2} + \frac{\partial \tau_{3i}}{\partial x_3} \zeta, \quad i = 1, 2, 3. \end{aligned} \quad (17)$$

The scattered amplitudes follow from the first-order perturbation equations in dependence on the amplitudes (16),

$$\mathbf{C}_s(B_r, B_p, B_t)^T = (D_1, D_2, D_3)^T, \quad (18)$$

where

$$\begin{aligned} D_1 &= i \left[ - \left( \frac{\omega^2}{c_w^2} - \mathbf{k}_0 \cdot \mathbf{k}_s \right) (A_0 + A_r) + \frac{\omega^2}{c_p^2} A_p - \mathbf{k}_0 \cdot \mathbf{k}_s \left( A_p - \frac{\gamma_{t0}}{k_0} A_t \right) \right], \\ D_2 &= i \left[ \rho_w \gamma_{w0} \omega^2 (A_0 - A_r) - \rho_b \gamma_{p0} \omega^2 A_p + 2\rho_b c_t^2 k_0^2 \left( \gamma_{p0} A_p - \frac{\gamma_{t0}^2}{k_0} A_t \right) \right], \\ D_3 &= \frac{i}{k_s} \left[ \rho_w \omega^2 (k_s^2 - \mathbf{k}_0 \cdot \mathbf{k}_s) (A_0 + A_r) + \rho_b k_s^2 \omega^2 \left( 2 \frac{c_t^2}{c_p^2} - 1 \right) A_p \right. \\ &\quad \left. + \rho_b (\omega^2 \mathbf{k}_0 \cdot \mathbf{k}_s - 2c_t^2 (\mathbf{k}_0 \cdot \mathbf{k}_s)^2) \left( A_p - \frac{\gamma_{t0}}{k_0} A_t \right) \right]. \end{aligned}$$

The matrix  $\mathbf{C}_s$  is obtained from (16) by replacing the index '0' by 's', with  $\mathbf{k}_s$  defined in (8). For further analysis, only the amplitude  $B_r$  is of interest.

In the limiting case of vanishing shear-velocity  $B_r$  becomes

$$B_r = 2i\gamma_{w0} A_0 \frac{(\alpha - 1)(\alpha(\mathbf{k}_0 \cdot \mathbf{k}_s - k_0^2) - \gamma_{p0}\gamma_{ps}) - \alpha(\alpha\gamma_{w0}^2 - \gamma_{p0}^2)}{(\alpha\gamma_{w0} + \gamma_{p0})(\alpha\gamma_{ws} + \gamma_{ps})}, \quad (19)$$

with  $\alpha = \rho_b/\rho_w$ .

Layered seafloor In order to investigate the influence of a layered seafloor on scattering, the simplest case is considered, i.e., a seafloor consisting of two sedimental

layers (without shear), both with constant sound velocity and density. While the upper layer is of constant depth the lower extends to infinity. Roughness is considered only at the seafloor, but not between the two bottom layers. The boundary conditions for both interfaces require continuity of normal particle velocity and pressure. In the case of no roughness (zero-order solution) an incident acoustic wave ( $A_0$ ) generates a reflected wave ( $A_r$ ) in the water column, a downwards ( $A_a^-$ ) and an upwards ( $A_a^+$ ) travelling wave in the upper sediment layer and a transmitted downwards travelling wave ( $A_b$ ) in the lower layer. By eliminating the latter amplitude from the boundary conditions, the other three are determined by

$$\mathbf{C}_0(A_r, A_a^-, A_a^+)^T = (-A_0, \rho_a \gamma_{w0} A_0, 0)^T, \quad (20)$$

where

$$\mathbf{C}_0 = \begin{pmatrix} 1 & -1 & -1 \\ \rho_a \gamma_{w0} & \rho_w \gamma_{a0} & -\rho_w \gamma_{a0} \\ 0 & (\rho_a \gamma_{b0} - \rho_b \gamma_{a0}) & (\rho_a \gamma_{b0} + \rho_b \gamma_{a0}) \exp(-2i\gamma_{a0}d) \end{pmatrix},$$

and where the indices 'a' and 'b' refer to the upper and lower sedimental layer, respectively, and  $d$  is the thickness of the upper layer.

The first-order perturbation is determined by the boundary conditions at the rough interface, which require continuity at  $x_3 = 0$  of

$$u_3 - u_1 \frac{\partial \zeta}{\partial x_1} - u_2 \frac{\partial \zeta}{\partial x_2} + \frac{\partial u_3}{\partial x_3} \zeta, \quad p + \frac{\partial p}{\partial x_3} \zeta. \quad (21)$$

The solution for the scattered amplitudes becomes

$$\mathbf{C}_s(B_r, B_a^-, B_a^+)^T = (D_1, D_2, 0)^T, \quad (22)$$

where

$$D_1 = i\gamma_{w0}(A_0 - A_r) - i\gamma_{a0}(A_a^- - A_a^+),$$

$$D_2 = i\rho_a(\mathbf{k}_0 \cdot \mathbf{k}_s - k_0^2 - \gamma_{w0}^2)(A_0 + A_r) - i\rho_w(\mathbf{k}_0 \cdot \mathbf{k}_s - k_0^2 - \gamma_{a0}^2)(A_a^- + A_a^+).$$

Again, only the amplitude  $B_r$  is of interest for further investigations.



---

### Numerical results for backscatter

---

Most available data are from backscatter. For this reason, the backscattering coefficient is of special interest. It is obtained by the condition

$$\mathbf{k}_s = -\mathbf{k}_0 \quad \text{i.e., } \vartheta_s = \vartheta_0, \varphi_s = \varphi_0 + 180^\circ. \quad (23)$$

Introducing the dimensionless and frequency-independent transfer function

$$T = \frac{|B_r|^2}{|\gamma_{w0} A_0|^2}, \quad (24)$$

the backscattering coefficient becomes, cf. (12),

$$S_B(\omega, \varphi_0, \vartheta_0) = \gamma_{w0}^4 T F(2\mathbf{k}_0), \quad (25)$$

as  $F(-\mathbf{k}) = F(\mathbf{k})$ . Inserting  $B_r$  from (19) for the limiting case of vanishing shear-velocity, (25) is identical to the formula used by Jackson et al. (1986).

The transfer function  $T$  depends on the geophysical properties of the sedimental seafloor, which are characterised by the velocity and attenuation of compressional and shear-waves and density. Parameters of some typical seafloor sediments from the continental shelf environment are presented in Table 1. These values are from Hamilton (1980) and represent averages. Attenuation is described by the imaginary part of the wave velocities, which implies a linear increase of attenuation with frequency. Shear-wave velocities are computed by means of a regression curve from compressional-wave velocities. With respect to water-saturated sediments at the seafloor, the values of shear-wave velocities may be too high. Attenuation has been taken from a seafloor model of Hamilton (1980) and refers to deeper sedimental layers.

Also, the parameters of Table 2 are from the seafloor model of Hamilton (1980), referring to a rigid seafloor consisting of consolidated sediments or rocks. The examples chosen cover shear-wave velocities from half to about double of the sound velocity of water.

The two-dimensional roughness spectrum  $F(\mathbf{k})$  depends on the absolute value and the direction of wavenumber. With respect to the directional dependence we assume for simplicity that the spectrum is isotropic,

$$F(\mathbf{k}) = \frac{G(k)}{2\pi k}, \quad (26)$$

**Table 1** *Seafloor parameters from the continental-shelf environment<sup>1</sup>*

Seafloor	$\rho_b/\rho_w$	$c_p/c_w$	$c_t/c_w$
silty clay	1.4	$0.99 - 0.002i$	$0.10 - 0.004i$
silt	1.7	$1.06 - 0.003i$	$0.23 - 0.03i$
very fine sand	1.85	$1.12 - 0.004i$	$0.28 - 0.05i$
coarse sand	2.0	$1.20 - 0.005i$	$0.32 - 0.07i$

<sup>1</sup>  $\rho_b$ ,  $\rho_w$  are the densities of seafloor and water,  $c_p$ ,  $c_t$  the compressional- and shear-wave velocity of the seafloor, and  $c_w$  the sound velocity in water.

**Table 2** *Seafloor parameters from rigid seafloors (for further explanation cf. Table 1)*

Seafloor	$\rho_b/\rho_w$	$c_p/c_w$	$c_t/c_w$
sedimentary rock	2.2	$1.4 - 0.006i$	$0.5 - 0.15i$
sedimentary rock	2.3	$1.7 - 0.003i$	$0.7 - 0.09i$
sedimentary rock	2.5	$2.3 - 0.004i$	$1.3 - 0.11i$
basalt	2.7	$3.4 - 0.006i$	$1.8 - 0.006i$

where  $G(k)$  is the one-dimensional wavenumber spectrum which is normalised by,  $\langle \zeta^2 \rangle = \int G(k) dk$ , cf. (5). Inserting (26) into (25) yields

$$S_B(\omega, \varphi_0, \vartheta_0) = \frac{\gamma_{w0}^4 T G(2k_0)}{4\pi k_0} \quad (27)$$

For computing scattering strengths we consider two different spectra,

$$G(k) = \begin{cases} G_0 k^{-3}, & \text{for } k \geq k_u \\ 0, & \text{for } k < k_u, \end{cases}$$

and

$$G(k) = \begin{cases} (2k_u)^{-1} G_0 k^{-2}, & \text{for } k \geq k_u \\ 0, & \text{for } k < k_u. \end{cases} \quad (29)$$

In both spectra (28) and (29),  $G_0$  is a dimensionless constant, and both spectra contain the same total variance,

$$\langle \zeta^2 \rangle = \frac{G_0^2}{2} k_u^{-2}. \quad (30)$$

Synthetic series of bottom roughness, as represented by the spectrum (28), are presented by Essen (1992).

SACLANTCEN SM-271

As  $T$  in (25) does not depend on frequency, the frequency dependence of the backscattering coefficient is determined by the factor  $\gamma_{w0}^4$  and by  $F(\mathbf{k})$ , with the first yielding a  $\omega^4$  dependence. By assuming an isotropic spectrum this dependence reduces to  $\omega^3$ , cf. (27). Thus, with spectrum (28) backscatter becomes independent of frequency, in accordance with most of the data presented by Bunchuk and Zhitkovskii (1980). Spectrum (29) yields a linear increase of backscatter with frequency. Some of the measurements summarised by Urick (1980) show this behaviour.

The spectra (28) and (29) contain two parameters, the amplitude  $G_0$  and the cutoff-wavenumber  $k_u$ . For later investigations we refer to the values

$$G_0 = 0.01 \quad \text{and} \quad k_u = \frac{2\pi}{0.5} m^{-1}. \quad (31)$$

The spectral amplitude has been chosen to yield realistic values of backscatter strength. The cutoff-wavenumber corresponds to the wavelength of 0.5 m and has been determined by the condition that it should be smaller than possible resonant wavenumbers, i.e., wavenumbers responsible for backscattering, which depend on the acoustic frequency and the grazing angle. Grazing angles considered are below  $75^\circ$ . For higher grazing angles specular reflections may become important, and perturbation theory fails. Acoustic frequencies are assumed to be above 10 kHz. From these conditions the maximum resonant wavenumber turns out to be about twice the cutoff-wavenumber in (31).

Figure 1 displays backscattering strength, i.e., the dB values of the scattering coefficient (27), as a function of grazing angle for the two spectra (28) and (29) with amplitude  $G_0$  and cutoff-wavenumber  $k_u$  from (31). For simplicity a homogeneous seafloor without attenuation and shear is considered. The solid line refers to the  $k^{-3}$  spectrum (28) with backscatter independent of frequency, as long as the resonant wavenumber exceeds the cutoff-wavenumber  $k_u$ . The dashed lines refer to the  $k^{-2}$  spectrum (29) which yields a linear increase of backscatter with frequency. The magnitude of backscatter is dependent on the cutoff-wavenumber  $k_u$ , cf. (29).

Though both spectra (28) and (29) contain equal total variance, backscattering strengths in Fig. 1 vary considerably. This means that backscatter may not be determined by the rms value of bottom roughness. The spectral density at the respective resonant wavenumber has to be known. The difference between (28) and (29) is the distribution of variance over the range of resonant wavenumbers.

Figure 2 compares backscattering strengths as obtained from a seafloor with shear and without shear. Spectrum (28) is used and sediment parameters are taken from Table 1 (solid lines). For the dotted lines shear-wave attenuation is ignored, and the dashed lines refer to a shear-free bottom. The influence of shear increases with the value of shear-wave velocity, but only affects grazing angles below critical. In the case of coarse sand (upper panel), the backscatter strength is less by more than 5 dB for small grazing angles. Shear-wave attenuation obviously is of minor importance.

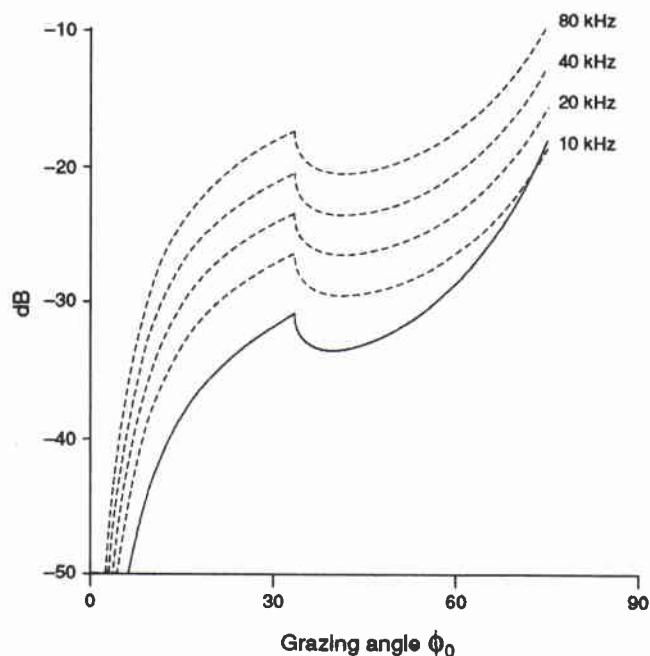


**Figure 1** Backscattering strength as a function of grazing angle, from a homogeneous fluid seafloor without attenuation, sediment parameters:  $\rho_b/\rho_w = 2.0$ ,  $c_b/c_w = 1.2$ , roughness spectrum (28): solid line, and (29): dashed lines, with  $G_0$  and  $k_u$  from (31).

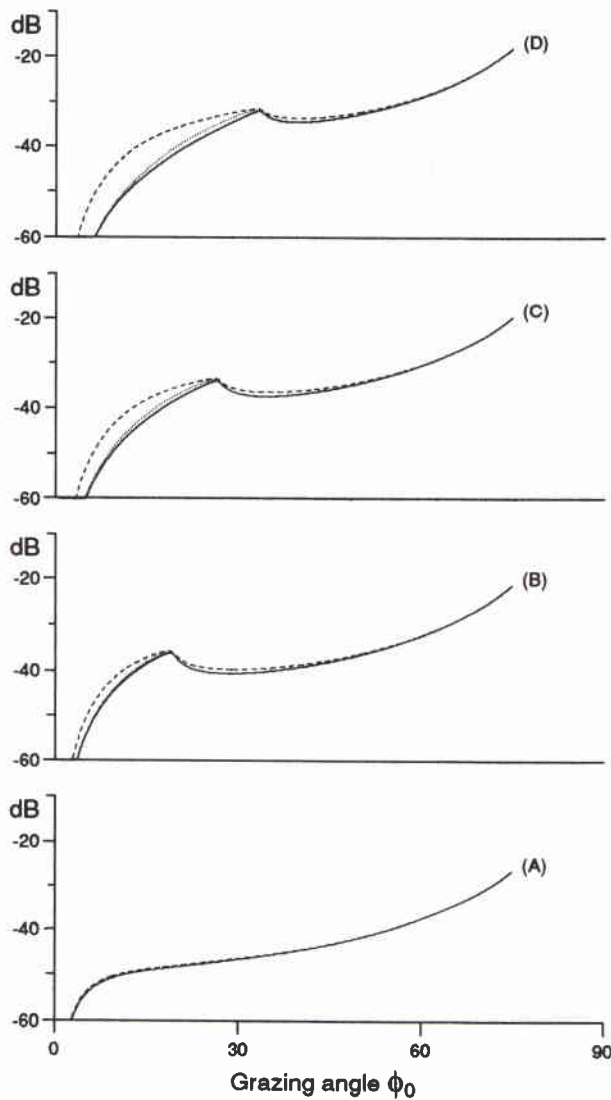
The same applies to compressional-wave attenuation, which is responsible for some smoothing of the cusp at critical angle, cf. Fig. 1.

Figure 3 displays scattering strengths as obtained from hard seafloors with parameters from Table 2. Comparing seafloors with shear (solid lines) and without shear (dashed lines), considerable differences in backscattering strength are visible. Shear-wave attenuation is relatively high for sedimentary rocks but much less for basalt (cf. Table 2). This explains the strong deviation of scattering curves for shear-wave attenuation considered (solid lines) or not (dotted lines) in (A)–(C), which is not present for (D). Compressional-wave attenuation, as given by Table 2, is of minor importance and not investigated here.

Figure 4 displays backscattering strengths as obtained for a two-layer fluid seafloor. Sediment parameters are those for silt (upper layer of thickness  $d$ ) and very fine sand (lower unbounded layer), cf. Table 1, and contain no shear. The four panels are for different  $d$ , which is assumed to be a multiple  $n$  of the acoustic wavelength  $\lambda = 2\pi c_w/\omega$ , with  $n = 0.2, 1, 5, 25$  (from below). The dashed line refers to backscatter strength from an unbounded silty seafloor. Due to the short acoustic penetration into the seafloor at angles below critical, there is also only little influence of layering on backscatter strength.

Considering case (A) in Fig. 4 with the layer thickness  $d$  being small compared to the acoustic wavelength  $\lambda$ , backscatter approaches that obtained from the sandy seafloor only, except for a factor of the squared impedance ratio of both layers, which is 1.2 dB for the parameters used in Fig. 4. It is remarkable that the cusp in the backscattering curve does not occur at the critical angle of the uppermost layer

## SACLANTCEN SM-271



**Figure 2** Backscattering strength as a function of grazing angle, from a (soft) seafloor containing shear (solid lines), seafloor parameters from Table 1: silty clay (A), silt (B), very fine sand (C), coarse sand (D), roughness spectrum (28) with  $G_0$  and  $k_u$  from (31). Dotted lines: zero shear-wave attenuation, dashed lines: no shear.

but at that of the underlying halfspace. Also for case (B), with layer thickness being equal to the acoustic wavelength, the critical angle of the lower halfspace dominates the curve's behaviour, with a notch of some 15 dB. For thicker layers (cases (C) and (D)), backscatter curves oscillate for angles above critical. The decrease of oscillation amplitudes with layer thickness is due to compressional wave attenuation.

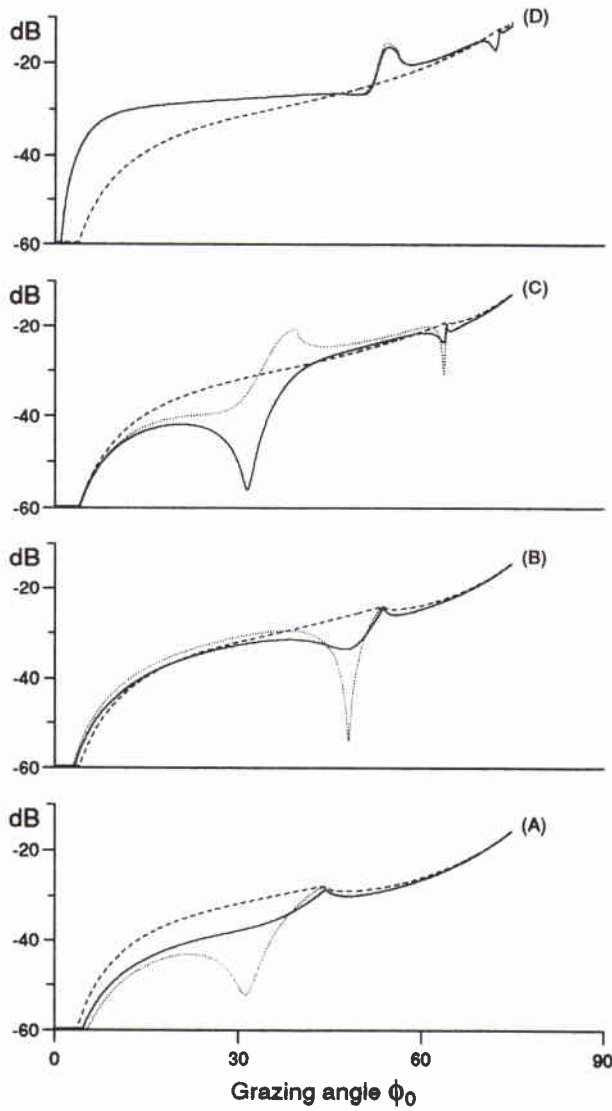


**Figure 3** Backscattering strength as a function of grazing angle, from a (hard) seafloor containing shear (solid lines), seafloor parameters from Table 2: sedimentary rocks (A)–(C), basalt (D), roughness spectrum (28) with  $G_0$  and  $k_u$  from (31). Dotted lines: zero shear-wave attenuation, dashed lines: no shear.

SACLANTCEN SM-271

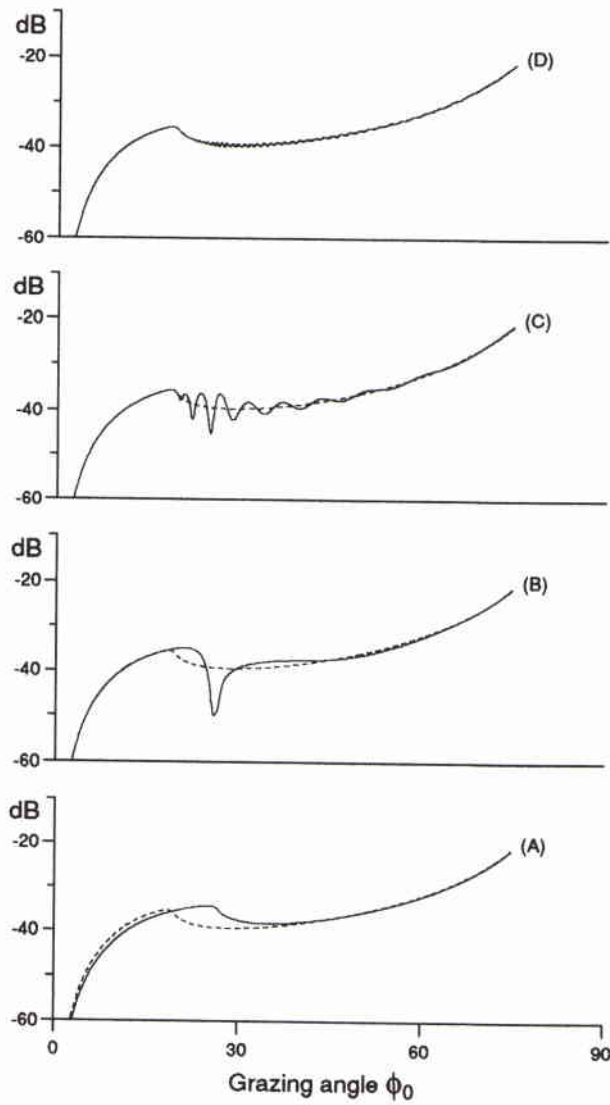


**Figure 4** Backscattering strength as a function of grazing angle, from a two-layer fluid seafloor (solid lines), with upper layer of thickness  $d$ : silt, lower layer: very fine sand, sediment parameters from Table 1 (without shear),  $d = n\lambda$  (acoustic wavelength),  $n = 0.2(A), 1(B), 5(C), 25(D)$ , roughness spectrum (28) with  $G_0$  and  $k_n$  from (31). Dashed lines: unlayered seafloor with parameters of the upper layer (silt).

## 4

## Numerical results for bistatic scattering

Analogous to the case of backscatter, we make use of the dimensionless and frequency-independent transfer function (24) and assume that the roughness spectrum is isotropic (26). Then, the scattering coefficient (12) becomes,

$$S(\omega, \varphi_s - \varphi_0, \vartheta_0, \vartheta_s) = \gamma_{w0}^2 \gamma_{ws}^2 T \frac{G(|\mathbf{k}_s - \mathbf{k}_0|)}{2\pi |\mathbf{k}_s - \mathbf{k}_0|}. \quad (32)$$

Due to the isotropic spectrum the scattering coefficient depends on the difference of scattered and incident azimuthal angle, only. The formula suggests a dependence of the bistatic scattering strength on grazing angles by  $(\sin \vartheta_0 \sin \vartheta_s)^n$  with  $n = 2$ , different from that derived by Ellis and Crowe (1991) from Lambert's Rule with  $n = 1$ . Some of this discrepancy is compensated by  $T$ , which depends on both grazing angles.

Figure 5 displays scattering strength as function of the difference of azimuthal angle  $\varphi_s - \varphi_0$ , which is  $0^\circ$  in the case of forward- and  $180^\circ$  in the case of backscattering. The parameters for coarse sand (cf. Table 1) have been used, and spectrum (28) with  $k^{-3}$  dependence. This spectrum yields frequency-independent scattering strengths. But the angle, at which the curves cut off in Fig. 5, depends on frequency, because it is determined by the cutoff-wavenumber  $k_u$  of the roughness spectrum (28). Two grazing angles are considered for both incident and scattered wave, one ( $20^\circ$ ) below the critical angle, the other ( $40^\circ$ ) above. Seafloors with shear (solid lines), zero shear-wave attenuation (dotted lines) and without shear (dashed lines) are considered.

In accordance with the results from backscatter, the largest difference between scattering strengths is found if incident and scattered grazing angle are below critical (Fig. 5, upper panel). If one of these angles is below and the other above critical, the difference between scattering strength from a seafloor with and without shear decreases (two middle panels) and becomes very small for both angles above critical (lower panel). Interchanging incident and scattered grazing angle does not affect scattering strength.

Scattering strength as function of azimuthal angle from a two-layer fluid seafloor is displayed in Fig. 6. As compared to Fig. 5, a higher acoustic frequency (20 kHz) has been chosen, which shifts the cutoff azimuthal angle to smaller values. The depth of the upper layer has been set to 5 times the acoustic wavelength. With fixed grazing angles, the vertical components of incident and scattered wavenumber remain constant as function of grazing angle and so do the differences in scattering



SACLANTCEN SM-271

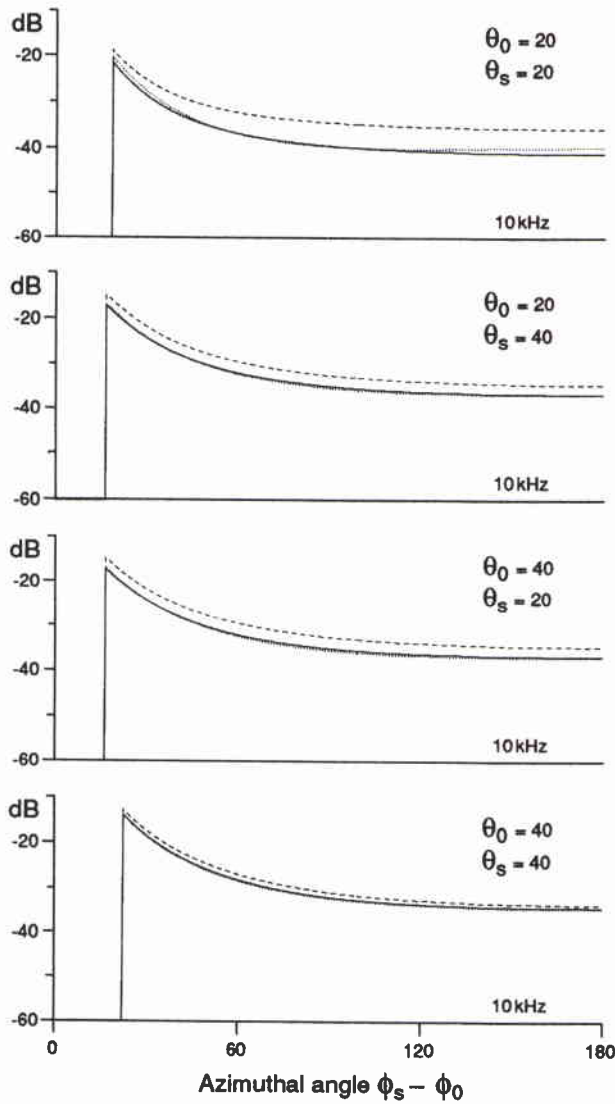


**Figure 5** Scattering strength (bistatic) as a function of azimuthal angle, for different incident and scattered grazing angles, from a seafloor containing shear (solid lines), seafloor parameters for coarse sand (cf. Table 1), roughness spectrum (28) with  $G_0$  and  $k_u$  from (31). Dotted lines: zero shear-wave attenuation, dashed lines: no shear. The low-angle cutoff depends on acoustic frequency (10 kHz).

strength of the two-layer (solid line) and the unlayered seafloor (dashed line). In general (Fig. 6, lower three panels), these differences are small, except in the case when one or both grazing angles correspond to maximum excursions of the oscillating backscattering strength (Fig. 4, upper panel).

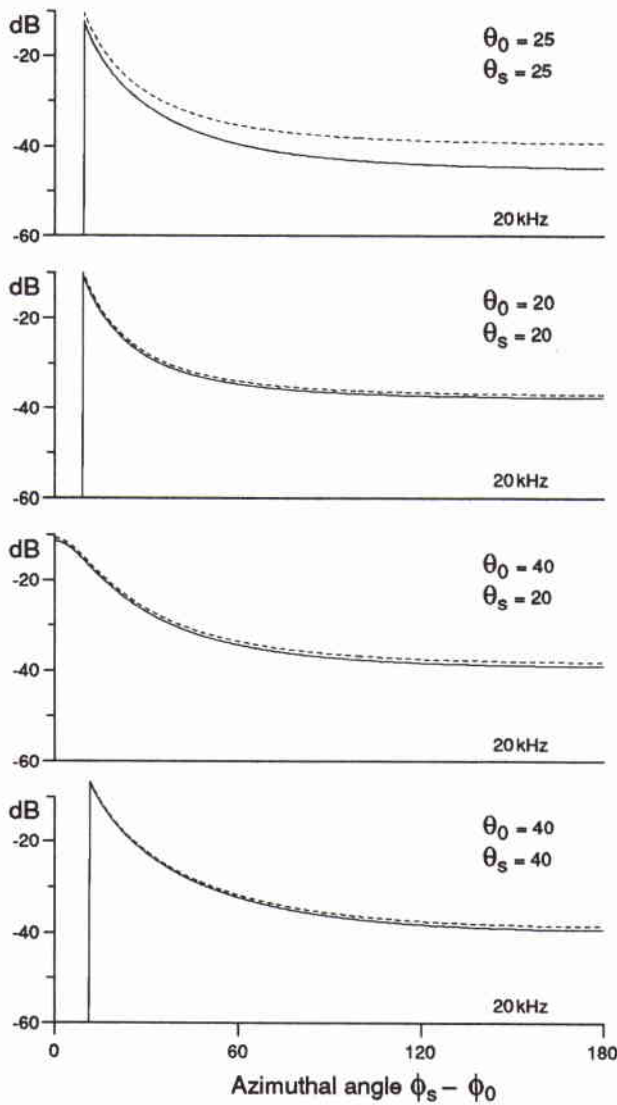


**Figure 6** Scattering strength (bistatic) as a function of azimuthal angle, for different incident and scattered grazing angles, from a two-layer fluid seafloor (solid line), with upper layer of thickness  $d$ : silt, lower layer: very fine sand, sediment parameters from Table 1 (without shear),  $d = 5\lambda$  (acoustic wavelength), roughness spectrum (28) with  $G_0$  and  $k_u$  from (31). Dashed lines: unlayered seafloor with parameters of the upper layer (silt). The low-angle cutoff depends on acoustic frequency (20 kHz).

## 5

## Conclusions

Scattering from a rough seafloor is one important mechanism in acoustic reverberation. Mainly for harder seafloors with compressional wave velocities exceeding the water sound velocity by more than a factor 1.1 (e.g. sand), first-order perturbation theory reasonably predicts observed backscatter data. The seafloor model used in the literature consists of an homogeneous fluid halfspace, characterised by density and compressional-wave velocity and attenuation. This model obviously oversimplifies reality. More realistic models should account for shear, which is to some extent always present, and layering. Both effects considerably complicate the boundary conditions.

Defining a deviation of more than 3 dB as significant, it may be stated that shear wave velocities higher than about  $350 \text{ ms}^{-1}$  significantly influence the scattering strength for grazing angles below critical. In unconsolidated sediments, shear-wave velocities are generally found to be slower, and shear may be ignored in scattering models. On the other hand, consolidated sediments and rocks contain higher shear-wave velocities. For limited ranges of grazing angle, differences of up to 20 dB occur between scattering strength from seafloors with and without shear. Furthermore, in consolidated sediments shear-wave attenuation is relatively high and considerably influences scattering strength.

Due to the short penetration of sound into the sediment for angles below critical, layering mainly affects grazing angles above critical. Above critical, scattering strength as a function of grazing angle shows oscillating features dependent on the ratio of layer depth to the vertical component of acoustic wavelength. For the example presented, amplitudes are of the order of 5 dB. This means that layering should be taken into account by interpreting observed data.

Perturbation theory may also be applied to bistatic scattering. For a roughness spectrum decaying with increasing wavenumber, the scattering geometry yields a decrease of scattering strength with increasing azimuthal scattering angle (measured from the specular direction). This decrease is strong for angles near specular but only weak for larger angles, qualitatively in accordance with experimental findings (cf. Ellis and Crowe, 1991). Due to the cutoff of the roughness spectrum at a given low wavenumber, as assumed in our investigations, scattering strengths are not obtained for grazing angles some  $20^\circ$  around specular direction.

Perturbation theory fails for grazing angles near normal incidence, and in the case of bistatic scattering for azimuthal angles near specular. In both cases, long bottom

waves become involved, and scattering is more reliably described by Kirchhoff's approximation. As most experimental data in the literature are from the frequency range 10–100 kHz, the investigations presented refer to this range. By simple scaling the theoretical results may also be applied to other frequency ranges (cf. Essen, 1992).

## References

---

- Boehme, H. and Chotiros, N.P. (1988). Acoustic backscattering at low grazing angles from the ocean bottom. *Journal of the Acoustical Society of America*, **84**, 1018-1029.
- Brekhovskikh, L. and Lysanov, Y. (1991). Fundamentals of Ocean Acoustics, 2nd ed. Berlin, Springer. [ISBN 3 540 52976 4]
- Bunchuk, A.V. and Zhitkovskii, Y.Y. (1980). Sound scattering by the ocean bottom in shallow-water regions (review). *Soviet Physics and Acoustics*, **26**, 363-370.
- Ellis, D.D. and Crowe, D.V. (1991). Bistatic reverberation calculations using a three-dimensional scattering function. *Journal of the Acoustical Society of America*, **89**, 2207-2214.
- Essen, H.-H. (1992). Perturbation theory applied to sound-scattering from a rough sea-floor, SACLANTCEN SR-194. La Spezia, Italy, NATO SACLANT Undersea Research Centre. [AD B 171 007]
- Hamilton, E.L. (1980). Geoacoustic modeling of the sea floor. *Journal of the Acoustical Society of America*, **68**, 1313-1340.
- Jackson, D.R. and Briggs, K.B. (1992). High-frequency bottom backscattering: roughness versus sediment volume scattering. *Journal of the Acoustical Society of America*, **92**, 962-977.
- Jackson, D.R., Winebrenner, D.P. and Ishimaru, A. (1986). Application of the composite roughness model to high-frequency bottom backscattering. *Journal of the Acoustical Society of America*, **79**, 1410-1422.
- Kuo, E.Y.T. (1964). Wave scattering and transmission at irregular surfaces. *Journal of the Acoustical Society of America*, **36**, 2135-2142.
- Mackenzie, K.V. (1961). Bottom reverberation for 530- and 1030-cps sound in deep water. *Journal of the Acoustical Society of America*, **33**, 1498-1504.
- Ogilvy, J.A. (1991). Theory of Wave Scattering from Random Rough Surfaces. Bristol, Adam Hilger. [ISBN 0 750 30063 9]
- Stanic, S., Briggs, K.B., Fleischer, P., Ray, R.I. and Sawyer, W.B. (1988). Shallow-water high-frequency bottom scattering off Panama City, Florida. *Journal of the Acoustical Society of America*, **83**, 2134-2144.
- Stanic, S., Briggs, K.B., Fleischer, P., Sawyer, W.B. and Ray, R.I. (1989). High-frequency acoustic backscattering from a coarse shell ocean bottom. *Journal of the Acoustical Society of America*, **85**, 125-136.
- Thorsos, E.I. (1990). Acoustic scattering from a Pierson-Moskowitz sea surface. *Journal of the Acoustical Society of America*, **88**, 335-349.
- Urick, R.J. (1983). Principles of Underwater Sound, 3rd ed. New York, NY, McGraw-Hill. [ISBN 0 07 066087 5]

<b>Security Classification</b> NATO UNCLASSIFIED		<b>Project No.</b> 23
<b>Document Serial No.</b> SM-271	<b>Date of Issue</b> July 1993	<b>Total Pages</b> 27 pp.
<b>Author(s)</b> H.-H. Essen		
<b>Title</b> Scattering from a rough sedimental seafloor containing shear and layering, as determined by perturbation theory		
<b>Abstract</b> First-order perturbation theory is applied to reverberation from a rough sedimental seafloor. In addition to existing approaches, the seafloor is allowed to be shear-supporting or to be layered. Scattering strengths are derived for both monostatic and bistatic reverberation, and compared with results from a non-layered fluid bottom. By exceeding some $350 \text{ ms}^{-1}$ , shear-wave velocity significantly influences scattering strength for angles below the critical angle of total reflection. Layering, as modelled by a two-layer fluid seafloor, mainly influences scattering at grazing angles just above critical.		
<b>Keywords</b> acoustic reverberation, layered seafloor, perturbation theory, rough seafloor, shear waves		
<b>Issuing Organization</b> North Atlantic Treaty Organization SACLANT Undersea Research Centre Viale San Bartolomeo 400, 19138 La Spezia, Italy [From N. America: SACLANTCEN CMR-426 (New York) APO AE 09613] tel: 0187 540 111 fax: 0187 524 600 telex: 271148 SACENT I		

### Initial Distribution for SM-271

SCNR for SACLANTCEN

SCNR Belgium	1
SCNR Canada	1
SCNR Denmark	1
SCNR Germany	1
SCNR Greece	1
SCNR Italy	1
SCNR Netherlands	1
SCNR Norway	1
SCNR Portugal	1
SCNR Spain	1
SCNR Turkey	1
SCNR UK	1
SCNR US	2
French Delegate	1
SECGEN Rep. SCNR	1
NAMILCOM Rep. SCNR	1

National Liaison Officers

NLO Belgium	1
NLO Canada	1
NLO Denmark	1
NLO Germany	1
NLO Italy	1
NLO Netherlands	1
NLO UK	3
NLO US	4
Total external distribution	30
SACLANTCEN Library	10
Stock	20
Total number of copies	60